Submitted to *Phys. Rev. D* ADP-98-4/T284
LTH 421

# Gluon Propagator in the Infrared Region

Derek B. Leinweber*, Jon Ivar Skullerud† and Anthony G. Williams‡
*Special Research Centre for the Subatomic Structure of Matter and The Department of Physics and Mathematical Physics, University of Adelaide, Adelaide SA 5005, Australia*

Claudio Parrinello§
*Department of Mathematical Sciences, University of Liverpool, Liverpool L69 3BX, England*

(UKQCD Collaboration)

## Abstract

The gluon propagator is calculated in quenched QCD for two different lattice sizes ($16^3 \times 48$ and $32^3 \times 64$) at $\beta = 6.0$. The volume dependence of the propagator in Landau gauge is studied. The smaller lattice is instrumental in revealing finite volume and anisotropic lattice artefacts. Methods for minimising these artefacts are developed and applied to the larger lattice data. New structure seen in the infrared region survives these conservative cuts to the lattice data. This structure serves to rule out a number of models that have appeared in the literature. A fit to a simple analytical form capturing the momentum dependence of the nonperturbative gluon propagator is also reported.

---

*E-mail: dleinweb@physics.adelaide.edu.au • Tel: +61 8 8303 3548 • Fax: +61 8 8303 3551
WWW: http://www.physics.adelaide.edu.au/theory/staff/leinweber/

†E-mail: jskuller@physics.adelaide.edu.au • Tel: +61 8 8303 3426 • Fax: +61 8 8303 3551
WWW: http://www.physics.adelaide.edu.au/~jskuller/

‡E-mail: awilliam@physics.adelaide.edu.au • Tel: +61 8 8303 3546 • Fax: +61 8 8303 3551
WWW: http://www.physics.adelaide.edu.au/theory/staff/williams.html

§E-mail: claudio@amtp.liv.ac.uk • Tel: +44 151 794 3775 • Fax: +44 151 794 3784
WWW: http://www.liv.ac.uk/TheoPhys/thep/people/cparrinello.html

## I. INTRODUCTION

The infrared behaviour of the nonperturbative gluon propagator has been the subject of extensive research and debate. Knowledge of this behaviour is generally regarded as being central to understanding the mechanism of confinement in quantum chromodynamics (QCD). Moreover, it is of great importance in various model-based approaches. For example, some studies based on Dyson–Schwinger equations [1–3] have indicated that an infrared enhanced gluon propagator may be required for confinement; however, others [4–6] have pointed to the possibility of a dynamically generated gluon mass, or other forms leading to an infrared finite (or even vanishing) propagator (see [7] and references therein).

Computing the gluon propagator directly on the lattice should provide an opportunity to resolve these contradictory claims. However, previous lattice studies [8,9] have been unable to access the "deep" infrared region where the most interesting nonperturbative behaviour is expected. Significant finite volume effects introduced through zero momentum components prevent the study of the infrared behaviour of the propagator on a small lattice.

The main aim of this study is to obtain a definite behaviour for the gluon propagator for momenta smaller than 1 GeV, where the interesting physics is expected to reside. In the following, we will report such results for momenta as small as 0.4 GeV. These momenta are small enough to reveal new structure in the gluon propagator and to place strong constraints on its infrared behaviour.

## II. THE GLUON PROPAGATOR ON THE LATTICE

The gauge links $U_\mu(x)$ may be expressed in terms of the continuum gluon fields as

$$U_\mu(x) = \mathcal{P} e^{ig_0 \int_x^{x+\hat\mu} A_\mu(z)dz} = e^{ig_0 a A_\mu(x+\hat\mu/2)} + \mathcal{O}(a^3)\,. \tag{2.1}$$

where $\mathcal{P}$ denotes path ordering. From this, the dimensionless lattice gluon field $A^L_\mu(x)$ may be obtained via

$$A^L_\mu(x+\hat\mu/2) = \frac{1}{2ig_0}\Big(U_\mu(x) - U^\dagger_\mu(x)\Big) - \frac{1}{6ig_0}\mathrm{Tr}\,\Big(U_\mu(x) - U^\dagger_\mu(x)\Big)\,, \tag{2.2}$$

which is accurate to $\mathcal{O}(a^2)$. Denoting the discrete momenta available on a finite, periodic volume by $\hat q$, the momentum space gluon field is

$$\begin{aligned} A_\mu(\hat q) &\equiv \sum_x e^{-i\hat q\cdot(x+\hat\mu/2)} A^L_\mu(x+\hat\mu/2) \\ &= \frac{e^{-i\hat q_\mu a/2}}{2ig_0}\left[\Big(U_\mu(\hat q) - U^\dagger_\mu(-\hat q)\Big) - \frac{1}{3}\mathrm{Tr}\,\Big(U_\mu(\hat q) - U^\dagger_\mu(-\hat q)\Big)\right], \end{aligned} \tag{2.3}$$

where $U_\mu(\hat q) \equiv \sum_x e^{-i\hat q x} U_\mu(x)$ and $A_\mu(\hat q) \equiv t^a A^a_\mu(\hat q)$. The available momentum values $\hat q$ are given by

$$\hat{q}_\mu = \frac{2\pi n_\mu}{aL_\mu}, \qquad n_\mu = 0, \ldots, L_\mu - 1 \tag{2.4}$$

where $L_\mu$ is the length of the box in the $\mu$ direction. The factor $e^{-i\hat{q}_\mu a/2}$, which comes from the gauge fields being defined on the links rather than the sites of the lattice, is crucial to removing $\mathcal{O}(a)$-errors and in particular obtaining the correct tensor structure for the gluon propagator [10]. The gluon propagator $D^{ab}_{\mu\nu}(\hat{q})$ is defined by

$$D^{ab}_{\mu\nu}(\hat{q}) \equiv \langle A^a_\mu(\hat{q}) A^b_\nu(-\hat{q})\rangle \,. \tag{2.5}$$

We choose to study the gauge dependent propagator in the Landau gauge, which can be implemented numerically by maximising $F[g] = \sum_{\mu,x} \Re\mathrm{Tr}\, U^g_\mu(x)$, where

$$U^g_\mu(x) = g(x)U_\mu(x)g^\dagger(x+\hat{\mu}). \tag{2.6}$$

In the continuum limit, this is related to the fact that fields satisfying the Landau gauge condition correspond to stationary points of $F^{cont}[g] = \| A^g \|^2 = \int d^4x \mathrm{Tr}\,(A^g_\mu)^2(x)$ [5].

The Landau gauge gluon propagator in the continuum has the form

$$D^{ab}_{\mu\nu}(q) = (\delta_{\mu\nu} - \frac{q_\mu q_\nu}{q^2})\delta^{ab} D(q^2)\,, \tag{2.7}$$

The scalar function $D(q^2)$ can then be extracted using

$$D(q^2) = \frac{1}{3}\sum_\mu \frac{1}{8}\sum_a D^{aa}_{\mu\mu}(q). \tag{2.8}$$

For $a \to 0$, the lattice propagator is related to the continuum one by $a^2 D(q^2) = D^{\mathrm{cont}}(q^2) + \mathcal{O}(a^2)$.

A well-known lattice artefact is that the tree level propagator of a massless boson field does not reproduce the expected continuum result of

$$D^{(0)}(q^2) = \frac{1}{q^2}, \tag{2.9}$$

but rather produces

$$a^2 D^{(0)}(\hat{q}) = \frac{a^2}{\sum_\mu (2\sin\hat{q}_\mu a/2)^2}\,. \tag{2.10}$$

In the following, we are particularly interested in the quantity $q^2 D(q^2)$, which is expected to approach 1 up to logarithmic corrections as $q^2 \to \infty$. To ensure this result we will work with the momentum variable defined as[1]

---

[1]The momenta $q$ and $\hat{q}$ are often defined the other way around in the lattice literature. However, we feel it is more instructive to define $q$ as above, such that lattice results reproduce the continuum formula (2.7) and the tree level formula (2.9).

$$q_\mu \equiv \frac{2}{a} \sin \frac{\hat{q}_\mu a}{2} \,. \tag{2.11}$$

## III. SIMULATION PARAMETERS

We have analysed 75 configurations at $\beta = 6.0$, on a $32^3 \times 64$ lattice. Using the value of $a^{-1} = 1.885$ GeV based on the string tension in [11], this corresponds to a physical volume of $(3.35^3 \times 6.70)$fm. For comparison, we have also studied an ensemble of 125 configurations on a smaller volume of $16^3 \times 48$, with the same lattice spacing.

The gauge configurations were generated using a combination of seven over-relaxation and one Cabibbo–Marinari updates, with a separation between configurations of 1000 combined updates for the large lattice and 800 for the smaller lattice. Both lattices were fixed to Landau gauge using a Fourier accelerated steepest descent algorithm [12]. An accuracy of $\frac{1}{VN_C}\sum_{\mu,x} |\partial_\mu A_\mu|^2 < 10^{-12}$ was achieved.

## IV. FINITE SIZE EFFECTS AND ANISOTROPIC BEHAVIOUR

### A. Small Lattice Analysis

We begin by considering the effect of the kinematic correction introduced through the change of variables in (2.11). In the absence of this correction, data in the high momentum region are expected to display significant anisotropy when shown as a function of $\hat{q}$. This is confirmed in Fig. 1, which shows the gluon propagator multiplied by $\hat{q}^2 a^2$ and plotted as a function of $\hat{q}a$. Here and in the following, a $Z_3$ averaging is performed on the data, where for example the momentum along (t,x,y,z) = (1,2,1,1) is averaged with (1,1,2,1) and (1,1,1,2).

We expect the kinematic correction to reduce anisotropy, particularly in the large momentum region. Fig. 2 shows the gluon propagator multiplied by the factor $q^2 a^2$ and plotted as a function of $qa$ for momenta directed throughout the lattice. The anticipated reduction of anisotropy for $qa > 1.5$ is nicely displayed in this figure. A similar result was found in [9].

Since the low momentum region holds the greatest nonperturbative interest, it is instructive to stress that the low momentum points displayed in Figs. 1 and 2 are insensitive to the whether one plots as a function of $q$ or $\hat{q}$. It is also useful to note that on any finite lattice, $D(q^2)$ will be finite at $q^2 a^2 = 0$. Hence any lattice calculation must give $q^2 a^2 D(q^2)$ vanishing at $q^2 = 0$.

On the small lattice, we also see significant anisotropy in the data which have their origin in finite volume artefacts. Finite size effects are expected to be largest where the momentum component along one or more of the lattice axes is zero. Since the length of the lattice in the time direction is three times that of the spatial directions, we notice a clear difference between points which correspond to momenta directed along spatial axes from those purely in the time direction. These finite volume artefacts are clearly displayed at small momenta

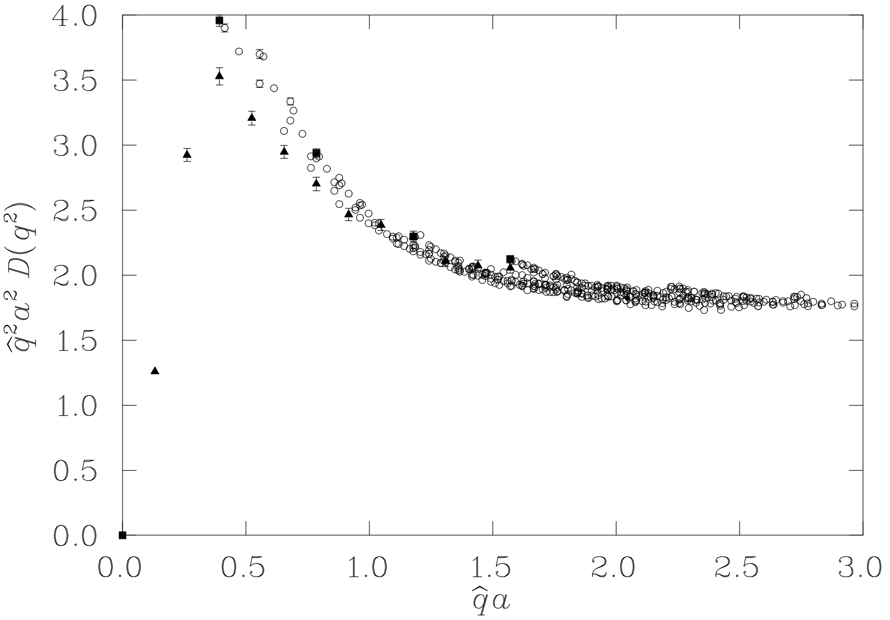


FIG. 1. The gluon propagator from our small lattice multiplied by $\hat{q}^2 a^2$ plotted as a function of momenta $\hat{q}a$. Values for each momentum direction are plotted separately. Only a $Z_3$ averaging has been performed. Filled squares denote momenta directed along spatial axes, while filled triangles denote momenta directed along the time axis. Other momenta are indicated by open circles.

by the discrepancies between the filled squares (denoting momenta directed along spatial axes), and the filled triangles (denoting momenta directed along the time axis).

Some residual anisotropy remains at moderate momenta around $qa \sim 1.5$ despite including the kinematical correction of (2.11). This anisotropy is clearly displayed in Fig. 2 by the filled squares and triangles denoting momenta directed along lattice axes lying below the majority of points from off-axis momenta[2] for $qa \sim 1.4$. Since tree-level and one-loop $O(4)$ breaking effects should be removed by the kinematical correction, the remaining anisotropy appears to have its origin in quantum effects beyond one loop.

In order to minimise lattice artefacts for large momentum components we select momentum vectors lying within a cylinder directed along the diagonal $(t, x, y, z) = (1, 1, 1, 1)$ of the lattice. This allows one to access the largest of momenta with the smallest of components. We found the selection of a cylinder with a radius of one spatial momentum unit ($\Delta \hat{q} a < 1{\times}2\pi/L_s$, where $L_s$ is the number of sites along a spatial axis) provides a reasonable number of points falling along a single curve for large momenta. The data surviving this

[2] In Fig. 2 it appears that this anisotropy disappears as one goes to even larger momenta. However, this is not necessarily the case. Only momentum components up to $\hat{q}_\mu a = 4 \times 2\pi/16$ have been selected in preparing Fig. 2. This means that the largest momenta are not accessed through any single Cartesian direction.

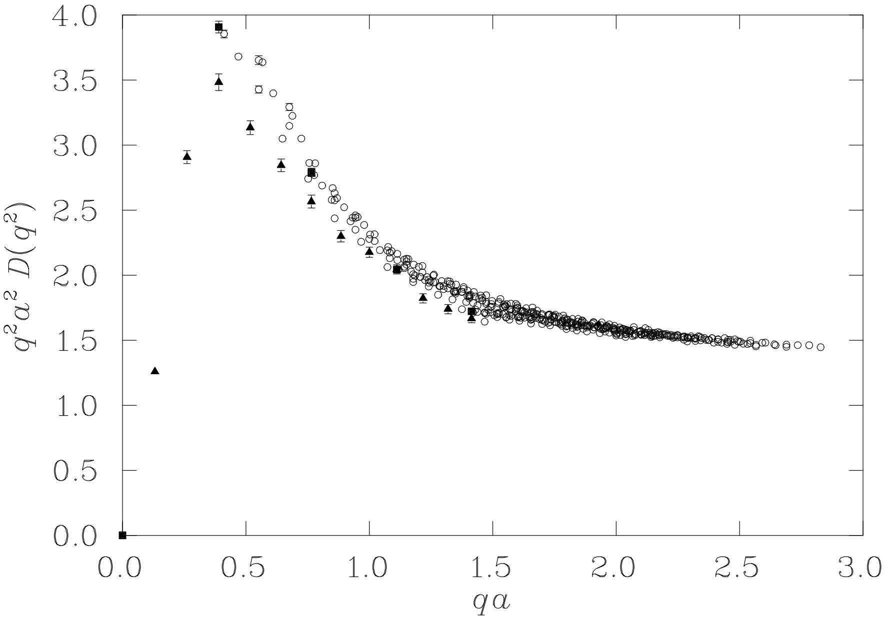


FIG. 2. The gluon propagator from our small lattice multiplied by $q^2a^2$ plotted as a function of momenta $qa$. Values for each momentum direction are plotted separately. Only a $Z_3$ averaging has been performed. The symbols are as in Fig. 1. Finite volume errors are expected to be largest for the purely time-like momenta, as the three shorter spatial directions have momentum components equal to zero and hence the effects of the nearby spatial boundaries are expected to be at a maximum.

cut are displayed in Fig. 3.

However, this cut does not address the large finite volume errors surviving in Fig. 3. To remove these problematic momenta, we consider a further cut designed to remove momentum vectors which have one or more vanishing components. This is implemented by keeping only momentum directions that lie within a certain solid angle of the diagonal. We found that a cone of angle 20° measured from the diagonal at the origin was sufficient to provide a set of points lying along a smooth curve. The solid points in Fig. 3 represent these data. After these conservative cuts, there is relatively little structure left in the infrared region on our small lattice. Armed with this knowledge of how to obtain reliable lattice data, we now turn our attention to the gluon propagator data obtained from our larger lattice.

### B. Large Lattice Analysis

Fig. 4 displays the gluon propagator data for all momentum directions and values on the larger lattice. Again, only a $Z_3$ averaging has been performed. Examination of the infrared region indicates that finite volume artefacts are very small on the larger lattice. In particular, the agreement between purely spatial (filled squares) and time-like momentum vectors (filled triangles) at $qa = 0.20$ appears to indicate that finite size effects are relatively

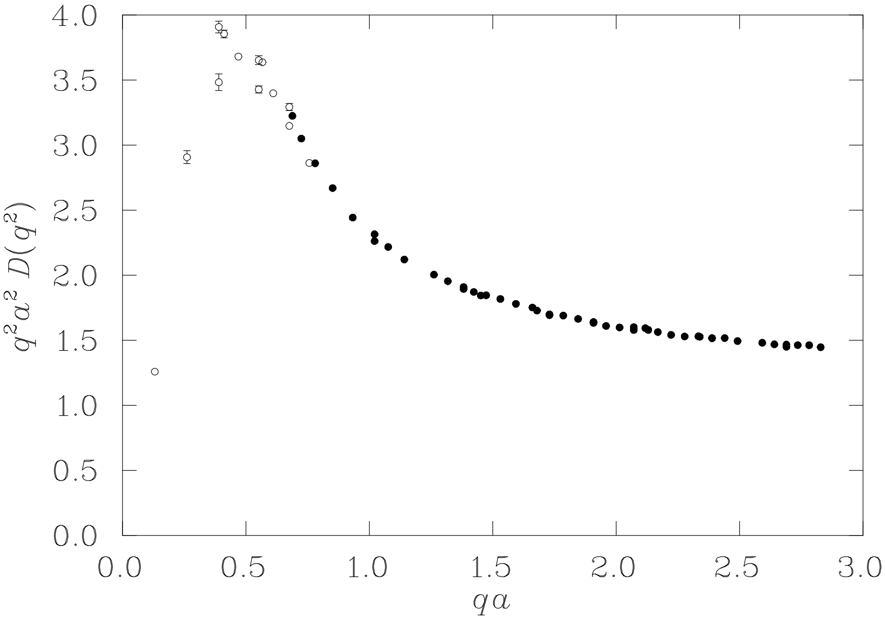


FIG. 3. The gluon propagator from our smaller lattice multiplied by $q^2a^2$. The points displayed in this plot lie within a cylinder of radius $\Delta\hat{q}a < 1\times 2\pi/16$ directed along the diagonal $(t,x,y,z) = (1,1,1,1)$ of the lattice. The solid points also lie within a cone of $20°$ measured from the diagonal at the origin.

small on this lattice. Such an observation is consistent with topological studies of the QCD vacuum which provide some insight into the typical scale of QCD vacuum fluctuations.

At large momenta, $qa > 1.0$, significant anisotropy is observed, similar to those displayed in Fig. 2. The fact that this anisotropy occurs at the same momentum values and with the same magnitude on both lattices confirms our previous argument that they result from finite lattice spacing errors as opposed to finite volume errors. Similar behaviour is expected in this region as the lattice action and lattice spacing are the same for our two lattices. To side-step this problem, we adopt the same cut as before. On this larger lattice, all momenta must lie within a cylinder of radius two spatial momentum units directed along the lattice diagonal. Fig. 5 displays the momenta surviving this cut.

While the two points at $qa = 0.20$ indicate that finite volume errors are small on this lattice, we also consider the additional angular cut, requiring that all points must lie within a cone of opening angle $20°$ from the diagonal at the origin. The data surviving this cautiously conservative cut are illustrated by the solid points in Fig. 5. It is interesting to see that the turnover in $q^2a^2\,D(q^2)$ in the infrared region survives even this extreme cut on our larger lattice.

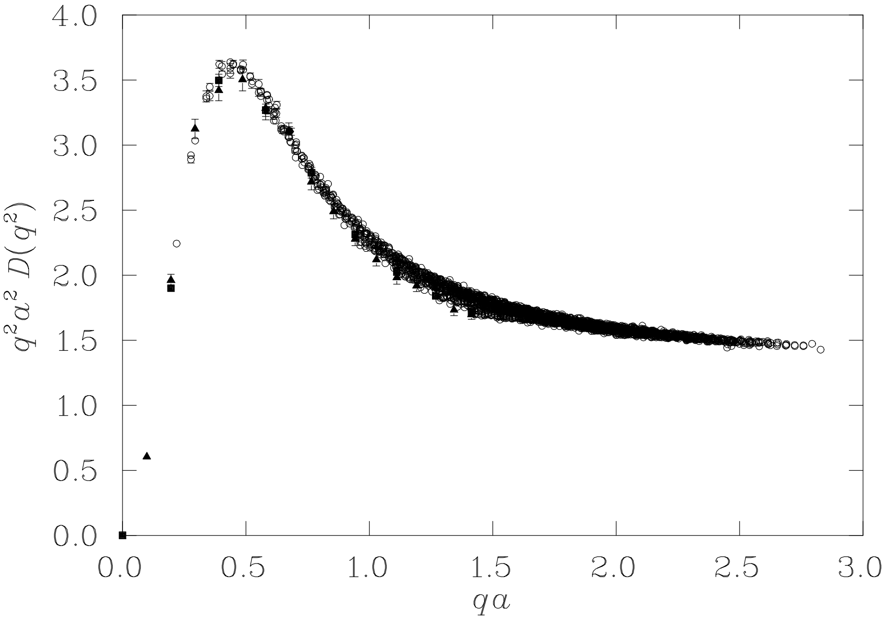


FIG. 4. The gluon propagator from our larger lattice multiplied by $q^2a^2$ plotted as a function of momenta $qa$. Values for each momentum direction are plotted separately. Only a $Z_3$ averaging has been performed for the data shown in this figure. Plotting symbols are as in Fig. 2. Finite volume errors are greatly reduced compared to the results from the smaller lattice, as displayed by the overlap of points obtained from spatial and time-like momentum vectors. However, significant anisotropy is apparent for larger momenta.

## V. MODELLING THE PROPAGATOR

The approach we have described here differs in several respects from that of [9]. In particular, the momentum vectors surviving our cuts are very different. In [9] only a small number of low-lying spatial momentum values are used along with all available time momentum values. In contrast, we have treated momenta in the spatial and time directions on an equal footing and selected momenta lying near the 4-dimensional diagonal, where lattice artefacts are expected to be minimal. In fact, nearly all the momenta used in [9] would be excluded by our cuts to the data.

In addition, we include the kinematical correction of (2.11). The authors of Ref. [9] do not include such a correction when performing their fits. Instead, their fits are constrained to the low-momentum region where such artefacts are hoped to be small.

We have considered a number of models for the propagator which have been suggested in the literature, as well as some simple analytical forms which are intended to capture the essence of the nonperturbative gluon propagator. A detailed analysis of these models is currently in progress [13].

The data for the fit are those obtained on the large lattice with the cylindrical cut. To balance the sensitivity of the fit over the available range of $qa$, we average adjacent lattice

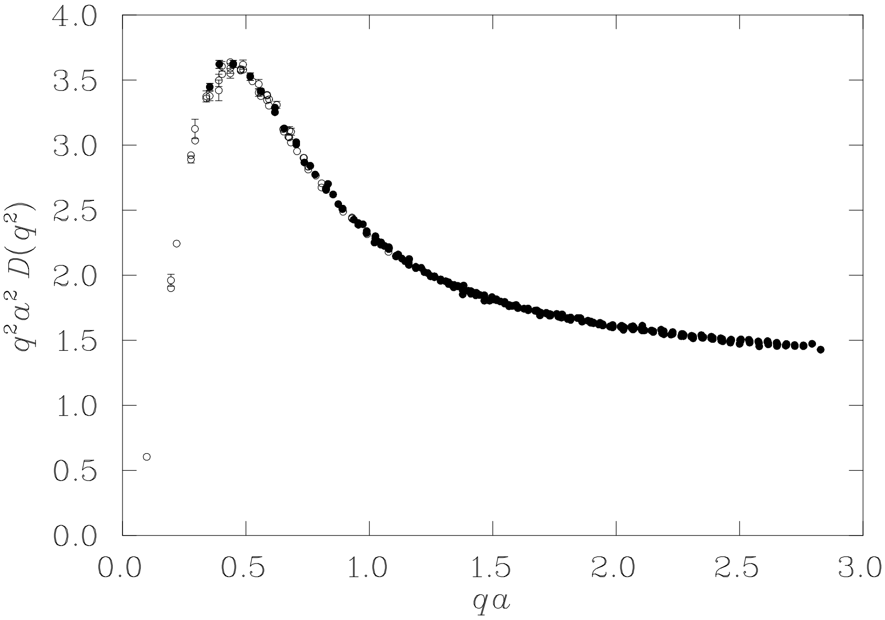


FIG. 5. The gluon propagator from our larger lattice multiplied by $q^2a^2$. The points displayed in this plot lie within a cylinder of radius $\Delta\hat{q}a < 2{\times}2\pi/32$ directed along the diagonal of the lattice. The solid points also lie within a cone of 20° measured from the diagonal at the origin. The first data point will be ignored in all fits, since it is not possible to assess the finite size effects for this point. The agreement between the next pair of data points indicates that finite size effects here are small.

momenta lying within $\Delta qa < 0.005$. In all fits the first point, at $qa \sim 0.1$, is omitted as it may be sensitive to the finite volume of the lattice.

Our results so far indicate that the following analytical form

$$D(q^2) = Z\left(\frac{A}{(q^2a^2)^{1+\alpha} + (M^2)^{1+\alpha}} + \frac{1}{q^2a^2 + M^2}\right) , \tag{5.1}$$

provides a satisfactory description of the data over a wide range of momenta. Our best fit to (5.1) is illustrated in Fig. 6.This fit yields $\chi^2/\mathrm{dof} = 3.5$, a somewhat high value. However, if the first four points are omitted, a more acceptable value of 1.6 is found.

We have studied the stability of the fits by varying the fitting range, and formula (5.1) turns out to give stable values for all the parameters over a wide region of fitting ranges. Our best estimates for the parameters, using all the available data, are

$$Z = 1.214^{+5+70}_{-5-25} \qquad A = 1.059^{+9+45}_{-9-65} \qquad \alpha = 0.784^{+4+80}_{-4-20} \qquad M = 0.375^{+2+50}_{-2-10}\, , \tag{5.2}$$

where the errors denote the uncertainties in the last digit(s) of the parameters. The first set of errors are statistical uncertainties in the fit to the full data set, and the second set of errors are due to fluctuations in the parameters as the fitting interval is varied. The estimate for $M$ corresponds to a physical value for the parameter in the region of 700 MeV.

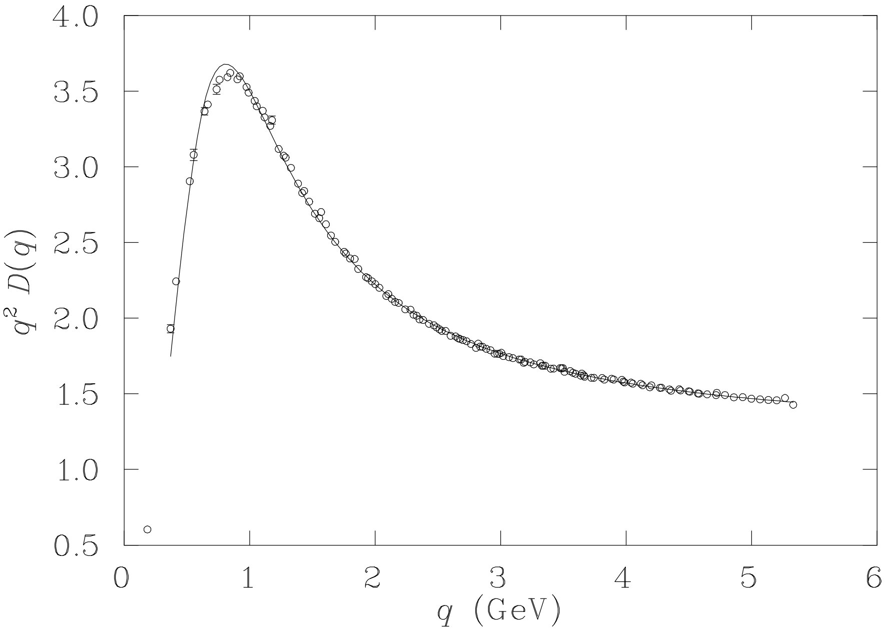


FIG. 6. The gluon propagator multiplied by $q^2$, with nearby points averaged. The line illustrates our best fit to the form defined in Eq. (5.1). The fit is performed over all points shown, excluding the one at the lowest momentum value, which may be sensitive to the finite volume of the lattice. The scale is taken from the value for the string tension quoted in [11].

## VI. CONCLUSIONS

We have performed an accurate, nonperturbative study of the infrared behaviour of the gluon propagator in the pure gauge theory on the lattice. We were able to isolate a set of data points for which systematic lattice errors seem to be negligible. Our data indicate an infrared behaviour less singular than $1/q^2$. This can be inferred from our plots by noticing the clear turnover in the behaviour of $q^2 a^2\, D(q)$ around $q^2 = 1$ GeV$^2$. This is in agreement with suggestions from previous lattice results. In particular, there is evidence that the nonperturbative gluon propagator may be infrared finite. Our data appear to rule out models like those proposed in [3], which lead to an infrared enhanced propagator.

Work in progress focuses on a detailed analysis of various analytic forms for the gluon propagator [13]. A stability analysis of the fit parameters is central to identifying the model best able to describe the gluon propagator in both the nonperturbative and the well known perturbative regimes. We are also exploring the possibility of extracting the value of $D(q = 0)$ in the infinite volume limit, which one may be able to extrapolate from data at different volumes. A study of the effects of Gribov copies [14] and a complete analysis of the tensor structure of the gluon propagator are also issues under consideration.

Finally, one promising line of research appears to be the study of the gluon propagator using improved lattice actions [15]. These should yield a significant reduction of finite lattice spacing effects. Then, by performing simulations at larger values of the lattice spacing, one would be able to measure the propagator on larger physical volumes, thus gaining access to very low momentum values. For example, one may be able to use lattice spacings as large as 0.4 fm, so that a modest $16^4$ lattice would have a physical size of 6.4 fm.

## ACKNOWLEDGMENTS

The numerical work was mainly performed on a Cray T3D based at EPCC, University of Edinburgh, using UKQCD Collaboration CPU time under PPARC Grant GR/K41663. Also, CP acknowledges further support from PPARC through an Advanced Fellowship. Financial support from the Australian Research Council is also gratefully acknowledged.

# REFERENCES


[1] S. Mandelstam, *Phys. Rev.* **D 20**, 3223 (1979)

[2] N. Brown and M.R. Pennington, *Phys. Rev.* **D 39**, 2723 (1989)

[3] M. Baker, J.S. Ball, F. Zachariassen, *Nucl. Phys.* **B 186**, 531 (1981)

[4] J. Cornwall, *Phys. Rev.* **D 26**, 1453 (1982)

[5] V.N. Gribov, *Nucl. Phys.* **B 139**, 19 (1978); D. Zwanziger, *Nucl. Phys.* **B 378**, 525 (1992); U. Habel et al, *Z. Phys.* **A 336**, 423 (1990)

[6] L. von Smekal, A. Hauck, R. Alkofer, *Phys. Rev. Lett.* **79**, 3591 (1997); D. Atkinson and J.C.R. Bloch, hep-ph/9712459 and hep-ph/9802239

[7] C.D. Roberts and A.G. Williams, *Progress in Particle and Nuclear Physics* **33**, 477-575 (1994)

[8] C. Bernard, C. Parrinello, A. Soni, *Phys. Rev.* **D49**, 1585 (1994)

[9] P. Marenzoni, G. Martinelli, N. Stella, *Nucl. Phys.* **B 455**, 339 (1995); P. Marenzoni, G. Martinelli, N. Stella, M. Testa, *Phys. Lett.* **B 318**, 511 (1993)

[10] B. Allés et al, *Nucl. Phys.* **B 502**, 325 (1997)

[11] G.S. Bali and K. Schilling, *Phys. Rev.* **D 47**, 661 (1993)

[12] C.T.H. Davies et al, *Phys. Rev.* **D 37**, 1581 (1988)

[13] D.B. Leinweber, C. Parrinello, J.I. Skullerud, A.G. Williams, in preparation.

[14] E. Marinari, C. Parrinello, R. Ricci, *Nucl. Phys.* **B 362**, 487 (1991); A. Cucchieri, *Nucl. Phys.* **B 508**, 353 (1997)

[15] K. Symanzik, *Nucl. Phys.* **B 226**, 187 (1983); M. Alford et al, *Phys. Lett.* **B 361**, 87 (1995)